The 3rd International Conference on Structural Health Monitoring of Intelligent Infrastructure
Vancouver, British Columbia, Canada
November 13-16, 2007

EMI-FREE MONITORING OF A RAILROAD BRIDGE FOR ELECTRIC POWERED LIGHT WEIGHT RAIL TRANSIT

Donghoon Kang
Korea Railroad Research Institute, Korea

Wonseok Chung
Korea Railroad Research Institute, Korea

Hyunmin Kim
Korea Railroad Research Institute, Korea

Inho Yeo
Korea Railroad Research Institute, Korea

Abstract

This paper investigates a prestressed concrete girder railroad bridge using FBG based sensors to monitor the dynamic response of the bridge with a test train which passes over the bridge at different speeds ranging from 10km/h to 50km/h. A test train made up of 2 cars is the Korean-standardized rubber-tired AGT (K-AGT) and it is powered by high-voltage of 22,900V. One FBG strain sensor and another FBG based accelerometer are attached on the surface of the bridge. For the comparison of measured data, an electric strain gage and an accelerometer are also attached near each FBG sensor. The results show that the measured data from FBG based sensors are free from EMI, though electric sensors are not, especially in the case of electric strain gage, which is crucial in the health monitoring of structures including high voltage power feeding systems.

INTRODUCTION

Among many types of light rail transits (LRT), the rubber-tired automated guide-way transit (AGT) vehicle has many advantages such as good acceleration and deceleration performance, high climbing capacity, and very low noise and vibration level due to rubber-tired wheels. For these reasons, the AGT system is very prevalent in modern railroad systems. However, it is generally powered by a high-voltage electric power feeding system and it can cause electromagnetic interference (EMI) to measurement sensors for structural health monitoring of railroad structures such as bridges, tunnels, and etc.

The fiber optic sensor system is free from EMI and has been successfully applied in many applications of civil engineering [1-2]. Especially, fiber Bragg grating (FBG) sensors are the most widely used because of its good multiplexing capabilities, that make it possible to reduce wiring dramatically, compared to the other fiber optic sensors.

In this paper, dynamic responses from two types of sensors (electric, fiber-optic) are compared when a test train passes over the prestressed concrete girder railroad bridge at different speeds ranging from 10km/h to 50km/h. A test train made up of 2 cars is the Korean-standardized rubber-tired AGT (K-AGT) and it is powered by high-voltage of 22,900V. On the surface of a test bridge, one FBG strain sensor and another FBG based accelerometer are attached and also with electric type sensors near them for the comparison. Through the whole test, the experimental data (strain, acceleration) from FBG based sensors are compared with those from conventional electric sensors.

DEMODULATION PRINCIPLE OF AN FBG SENSOR

The fiber Bragg grating has periodic changes of refractive index that are formed in the core of an optical fiber by the exposure of an intense UV interference pattern. This grating structure results in the reflection of the light at a specific narrowband wavelength, called the Bragg wavelength. The Bragg condition is given by $\lambda_B = 2\, n_e \Lambda$ where λ_B is the Bragg wavelength of FBG, n_e is the effective index of the fiber core, and Λ is the grating period. The wavelength, which is determined by the Bragg condition, reflects at the Bragg grating part and the other wavelengths pass through it [3]. Figure 1 shows this process.

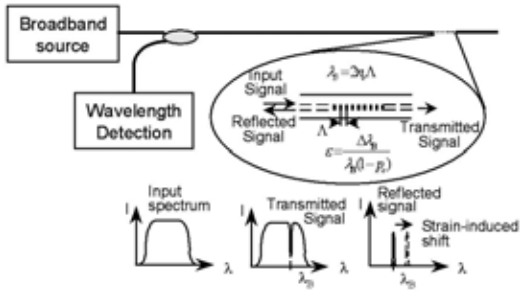

Figure 1. Fiber Bragg grating sensor wavelength-encoding operation.

In the Bragg condition, the Bragg wavelength is a function of the effective refractive index of the fiber core and the grating period. If the grating is exposed to the external environment such as strain and temperature, the Bragg wavelength changes. By measuring the wavelength change accurately, we can measure material properties like strain and temperature and this is the fundamental principle that fiber Bragg grating can be used as a sensor. The shift of Bragg wavelength due to strain and temperature can be expressed as

$$\Delta\lambda_B = \lambda_B\left[\left(\alpha_f + \xi_f\right)\Delta T + \left(1 - p_e\right)\varepsilon\right] \qquad (1)$$

where α_f is the coefficient of thermal expansion (CTE), ξ_f is the thermo-optic coefficient, and p_e is the strain-optic constant of the optical fiber. The value of p_e(=0.227) was measured experimentally and used for this study. If there is no temperature change, we can measure the strain from the wavelength shift as

$$\varepsilon = \frac{1}{1 - p_e}\frac{\Delta\lambda_B}{\lambda_B} \qquad (2)$$

From Eq. 2, the strain can be easily calculated just by measuring the wavelength shift. Also, we can measure the strains at many positions in single optical fibers by multiplexing capabilities of FBG sensors, because FBG sensors which have different Bragg wavelengths, do not influnce one another.

FIELD TEST PROGRAM

The configuration of a test train (K-AGT) is depicted in Fig. 2 and the test bridge in Fig. 3.

Figure 2. The test train (K-AGT).

Figure 3. A view of the bridge (PSC bridge).

The test bridge is a typical simple span prestressed concrete girder bridge with a length of 30 m. The superstructure consists of two girders built compositely with reinforced concrete slabs. The depth of the bridge is 2 m and the slab thickness is 250 mm. The detailed specifications are shown in Fig. 4.

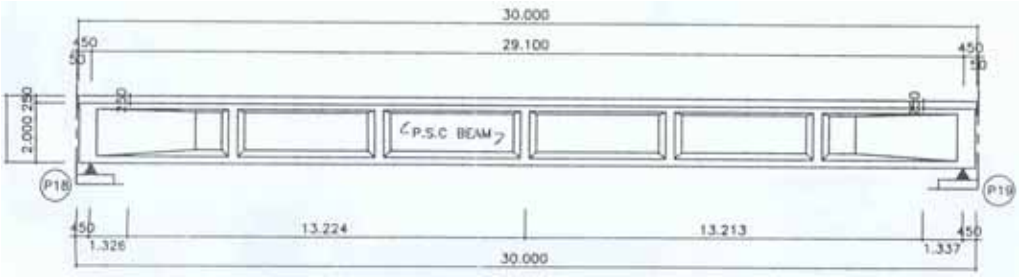

Figure 4. Details of girder.

Several FBG sensors are directly attached to the surface of the structure using epoxy glue. In addition to the FBG sensors, conventional electric strain gauges (ESG), LVDTs, and accelerometers are installed at the same locations for comparisons. As can be seen in Fig. 5, FBG sensors are installed on the bottom flange and on the upper surface of the side wall along the mid-span. It should be noted that the monitoring of the side wall is important because the K-AGT train moves along the rail that attaches along the side wall.

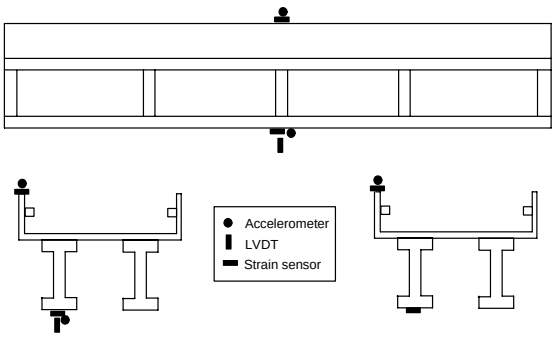

Figure 5. Sensor types and the locations.

In order to evaluate dynamic characteristics of the test bridge, the modal test is conducted as a part of the field test program. An FBG-based accelerometer is used to pick up the response of the test bridge. Two surface-mounted accelerometers were also installed at the mid-span, as shown in Fig. 5. Both an FBG accelerometer and a traditional accelerometer were installed at the same location (at mid-span) for comparisons. The FBG-based accelerometer used in this study (BPS-700, Tokyo Sokushin Co.) consists of a cantilever beam, a mass, a spring, and an FBG element, as shown in Fig. 6. This system is modeled by an un-damped, Single-Degree-of-Freedom (SDOF) system. A more detailed description of an FBG-based accelerometer is available in [4].

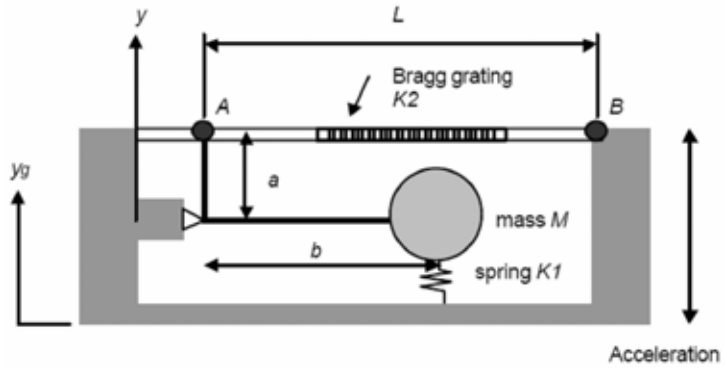

Figure 6. FBG-based accelerometer.

The test train is a K-AGT light weight train with a total weight of 115.8 kN. The detailed axle position is given in Fig. 7. Since the purpose of the test is to monitor the dynamic behavior of the bridge, the test train passes over the bridge at different constant speeds ranging from 10 km/h to 50 km/h with 10 km/h increments.

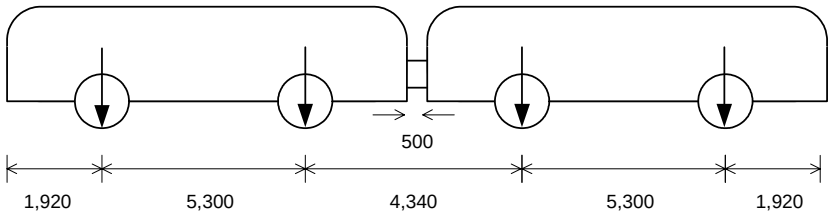

Unit : [mm]

Figure 7. Axle load model of the K-AGT.

TEST RESULTS

Figure 8 shows the comparisons of measured strains when the train passed the bridge at a speed of 10 km/h. The measuring frequency for the dynamic load test was 200 Hz. It is clear that the passing train induces compressive strains in the upper side wall and tensile strains in the bottom flange. Significant electric noise due to nearby high electric power system is observed in electric strain gauges. From Fig. 9 to Fig. 10, the strains obtained from the FBG sensor are compared with those from the electric resistance gauge for the train speeds of 30km/hr and 50km/hr. It is clear that the FBG sensors are free from electric noise and show clear strain signals during the test while the electric strain gauges are not free from noise.

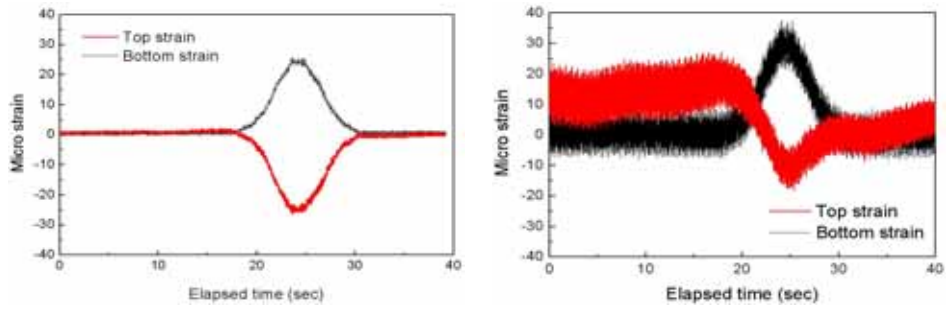

(a) FBG Sensor (b) Strain gauge

Figure 8. Strains for vehicle running at 10km/h.

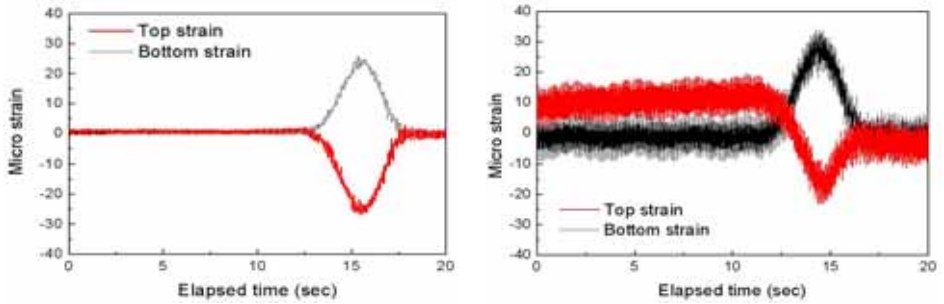

(a) FBG Sensor (b) Strain gauge

Figure 9. Strains for vehicle running at 30km/h.

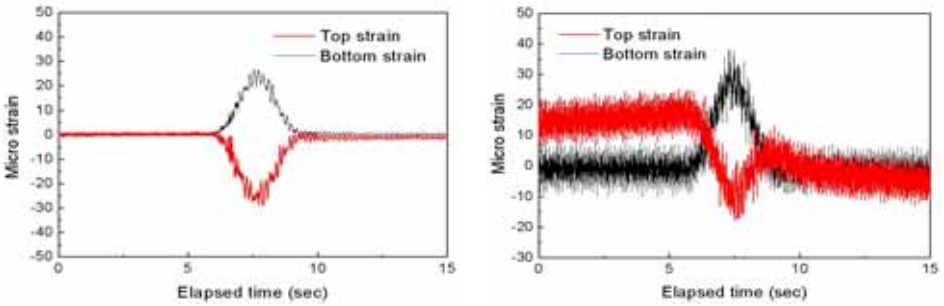

(a) FBG Sensor (b) Strain gauge

Figure 10. Strains for vehicle running at 50km/h.

Figures 11 to 13 show comparisons of the acceleration measured from the FBG-based accelerometer with those from the conventional accelerometer at the mid-span. The FBG-based accelerometer produces results close to a conventional accelerometer for all cases. The maximum measured acceleration differences between two accelerometers are 6%, 3%, and 13% for the three test cases.

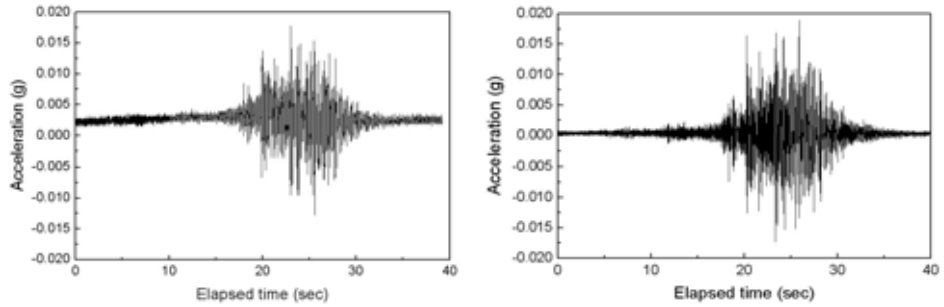

a) FBG-based accelerometer (b) Electric type accelerometer

Figure 11. Acceleration in a vehicle running at 10km/h.

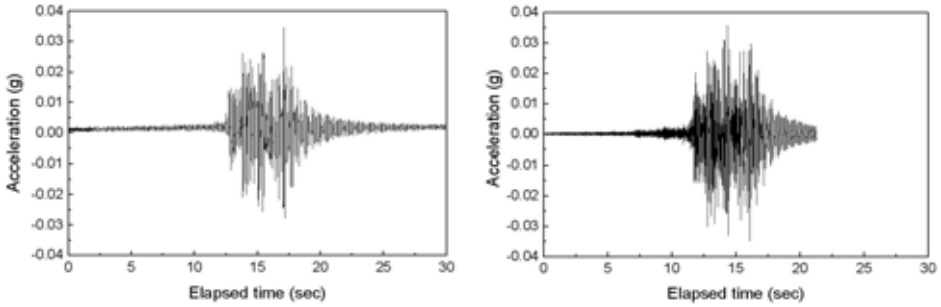

a) FBG-based accelerometer (b) Electric type accelerometer

Figure 12. Acceleration in a vehicle running at 30km/h.

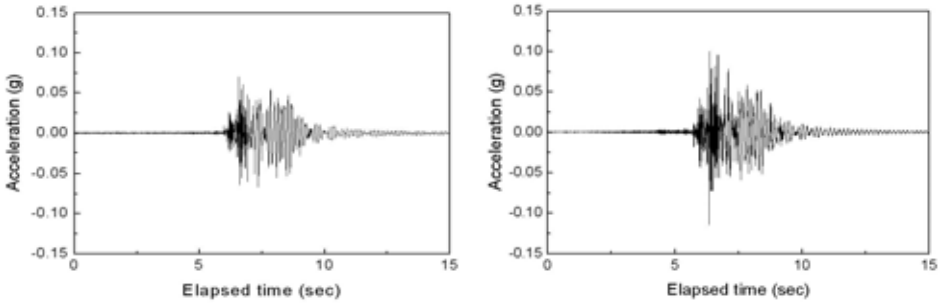

a) FBG-based accelerometer (b) Electric type accelerometer

Figure 13. Acceleration in a vehicle running at 50km/h.

Next, the test bridge is to evaluate natural frequencies using a commercial FBG based accelerometer. From the frequency analysis on the time history of response acceleration data under the vertical impact load, the extracted natural frequency of the first bending mode is 5.664 Hz when using the FBG-based accelerometer and 5.676 Hz for the conventional one, as shown in Fig. 14. Thus, the FBG-based accelerometer is able to trace the dynamic response of the bridge very well.

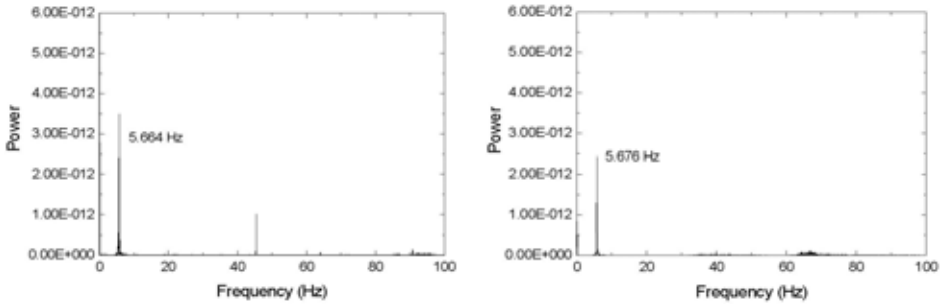

a) FBG-based accelerometer (b) Electric type accelerometer

Figure 14. Comparison of natural frequencies.

The maximum values measured from available sensors at each speed are given in Table 1. As the speed of the test train increases, the results show an insignificant increase in the maximum deflection. The increase in deflection is 9% for LVDT as the train speed increases five times from 10km/h to 50 km/h. It is because the natural frequency of the bridge was not in resonance with the driving frequencies of the train up to 50 km/h.

Table 1. Maximum values measured from available sensors at each speed

Vehicle Speed (km/h)	Deflection (mm)	Strain (με) (upper span)		Strain (με) (lower span)		Acceleration (g) (upper span)		Acceleration (g) (lower span)
		Electric	FBG	Electric	FBG	Electric	FBG	
10	1.23	36	26	-18	-26	0.016	0.015	0.010
20	1.25	35	25	-26	-28	0.026	0.031	0.020
30	1.31	32	26	-22	-26	0.032	0.031	0.022
40	1.28	31	25	-24	-27	0.056	0.048	0.025
50	1.36	38	27	-16	-28	0.077	0.067	0.046

CONCLUSIONS

This paper presents the feasibility of an FBG sensing system to a modern railway bridge that suffered from electric noise. First, a test train is passed over the bridge at different constant speeds so as to monitor the dynamic response of the bridge. The dynamic properties of the test girder are then identified using an FBG-based accelerometer. It was found that the FBG sensing system is capable of measuring the dynamic properties effectively. Moreover, the FBG sensors successfully captured the strain signal without electro-magnetic interference while electric strain gauges show significant noise in strain response. The success of the test encourages the use of the FBG sensing system as an alternative to a conventional system based on electric-type sensors. It is expected that the FBG sensing system can be effectively applied to the modern railway bridges that suffered from electro-magnetic interference.

REFERENCES

1. Chung, W.S., Kang, D.H., Choi, E.S. and Kim, H.M., 'Monitoring of a steel plate girder railroad bridge with fiber Bragg grating sensors', KSSC. 17(6)(2005) 681-688.

2. Chung, W.S., Kim, S.I., Kim, N.S. and Lee, H.U. 'Deflection estimation of a PSC railroad girder using long-gauge fiber optic sensors', KSR. 9(4)(2006) 467-472.

3. Udd, E., 'Fiber optic smart structures', (John Wiley and Sons, New York, 1995).

4. Mita, A and Yokol, I., 'Fiber Bragg grating accelerometer for structural health monitoring', Proceedings of 5th International Conference on Motion and Vibration Control, Sydney, Australia, 2000.